J. Biochem. **144,** 267–277 (2008)
doi:10.1093/jb/mvn065

An O^6-methylguanine-DNA Methyltransferase-like Protein from *Thermus thermophilus* Interacts with a Nucleotide Excision Repair Protein

Rihito Morita[1], Noriko Nakagawa[1,2], Seiki Kuramitsu[1,2] and Ryoji Masui[1,2,*]

[1]Department of Biological Sciences, Graduate School of Science, Osaka University, 1-1 Machikaneyama-cho, Toyonaka, Osaka 560-0043; and [2]RIKEN SPring-8 Center, Harima Institute, 1-1-1 Kouto, Sayo-cho, Sayo-gun, Hyogo 679-5148, Japan

Received March 6, 2008; accepted May 2, 2008; published online May 15, 2008

The major damage to DNA caused by alkylating agents involves the formation of O^6-methylguanine (O^6-meG). Almost all species possess O^6-methylguanine-DNA-methyltransferase (Ogt) to repair such damage. Ogt repairs O^6-meG lesions in DNA by stoichiometric transfer of the methyl group to a cysteine residue in its active site (PCHR). *Thermus thermophilus* HB8 has an Ogt homologue, TTHA1564, but in this case an alanine residue replaces cysteine in the putative active site. To reveal the possible function of TTHA1564 in processing O^6-meG-containing DNA, we characterized the biochemical properties of TTHA1564. No methyltransferase activity for synthetic O^6-meG-containing DNA could be detected, indicating TTHA1564 is an alkyltransferase-like protein. Nevertheless, gel shift assays showed that TTHA1564 can bind to DNA containing O^6-meG with higher affinity (9-fold) than normal (unmethylated) DNA. Experiments using a fluorescent oligonucleotide suggested that TTHA1564 recognizes O^6-meG in DNA using the same mechanism as other Ogts. We then investigated whether TTHA1564 functions as a damage sensor. Pull-down assays identified 20 proteins, including a nucleotide excision repair protein UvrA, which interacts with TTHA1564. Interaction of TTHA1564 with UvrA was confirmed using a surface plasmon resonance assay. These results suggest the possible involvement of TTHA1564 in DNA repair pathways.

Key words: DNA repair, methyltransferase, nucleotide excision repair, O^6-methylguanine, Ogt.

Abbreviations: 2AP, 2-aminopurine; AGT, O^6-alkylguanine-DNA alkyltransferase; ATL protein, alkyltransferase-like protein; dsDNA, double-stranded DNA; DTT, dithiothreitol; hMGMT, MGMT from Homo sapiens; MBP, maltose-binding protein; MGMT, O^6-methylguanine-DNA methyltransferase; MJOgt, Ogt from Methanocaldococcus jannaschii; NER, nucleotide excision repair; O^6-meG, O^6-methylguanine; Ogt, O^6-methylguanine-DNA methyltransferase; ssDNA, single-stranded DNA; TRCF, transcription-repair coupling factor; TTHB8, Thermus thermophilus HB8; WT, wild-type.

A great amount of DNA damage arises from both endogenous and exogenous DNA-damaging agents, for example, alkylating agents (*1*). O^6-alkylguanine is one such lesion with potent toxicity and potential for mutagenesis. Because O^6-alkylguanine forms hydrogen bonds with thymine in preference to cytosine, this lesion usually leads to GC-to-AT transition mutations (*2–4*). Among O^6-alkylguanine lesions, O^6-methylguanine (O^6-meG) is the major mutagenic lesion produced by simple methylating agents. O^6-alkylguanine is generated by antitumor alkylating agents and could also be formed by *S*-adenosylmethionine. The enzymes involved in repair of O^6-alkylguanine lesions play an important role in cellular drug resistance. Indeed, the phenomenon of cellular drug resistance is directly correlated to the intracellular level of these enzymes (*5*, *6*).

*To whom correspondence should be addressed. Tel: +81-6-6850-5434, Fax: +81-6-6850-5442,
E-mail: rmasui@bio.sci.osaka-u.ac.jp

O^6-meG is repaired by O^6-methylguanine-DNA methyltransferase (Ogt or MGMT), which accepts an alkyl group on a cysteine residue at the active site (PCHR) in a stoichiometric fashion (*7–9*). Transfer of the alkyl group results in the suicidal inactivation of Ogt. Ogt acts as a monomer and can transfer the alkyl group in the absence of any cofactor (*10–12*). Some Ogt homologues of other species are called O^6-alkylguanine-DNA alkyltransferases (AGTs), and the crystal structure of a human AGT has been reported (*13*, *14*). The structure of human AGT reveals that a helix-turn-helix motif mediates binding to the minor groove of DNA, and that O^6-meG is flipped out from the base stack into the active site. The structural data supports the idea that methylated nucleotide flipping is mediated by a tyrosine and arginine residues in the active site of the enzyme. Therefore, it has been generally accepted that AGT recognizes O^6-meG in DNA with nucleotide flipping (*13*, *14*).

Although AGT and Ogt homologues have been found in a wide range of organisms, several species possess no such homologue. Instead, Ogt-like proteins that lack a cysteine residue in their putative active site have been

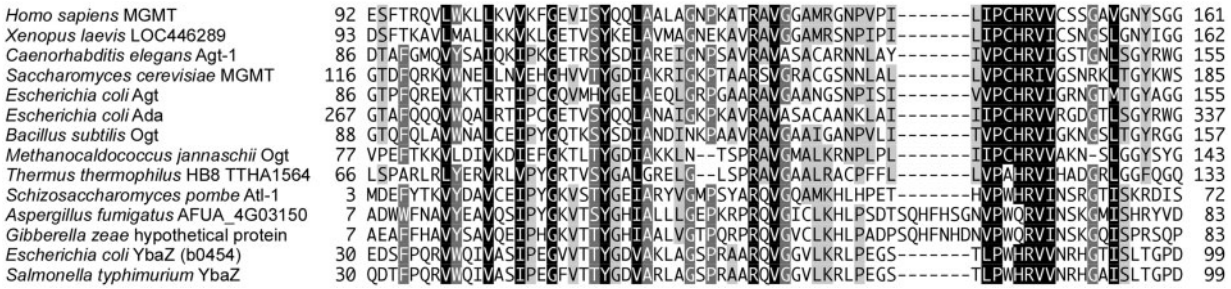

Fig. 1. **Amino acids sequence of homologous methyltransferase proteins and alkyltransferase-like proteins.** Sequences around the cysteine residue in the active site are aligned.

identified. In many instances the cysteine residue is replaced by tryptophan (PWHR; Fig. 1) (*15*). These Ogt-like homologues are called ATL (alkyltransferase-like) proteins and they are found in a broad range of prokaryotic species as well as eukaryotes such as *Schizosaccharomyces pombe* and several fungi. Interestingly, several species (e.g. *Escherichia coli*) possess both Ogt and ATL protein, whereas others (e.g. *S. pombe*) have only ATL protein. Some preliminary characterization of ATL protein from *E. coli* and *S. pombe* has already been reported (*15–17*). These proteins can bind both DNA and DNA containing O^6-meG. However, due to a paucity of quantitative data, it is unclear whether ATL protein has a higher affinity for O^6-meG-containing-DNA over normal (unmethylated) DNA. Intriguingly, although ATL protein lacks methyltransfer activity in the presence of O^6-methylguanine DNA, deletion of the ATL gene in *S. pombe* increases the sensitivity of the cells to methylating agents (*16*). Indeed, wild-type (WT) *S. pombe* has the ability to survive alkylation damage. Thus, it is unclear how ATL protein, which lacks methyltransferase activity, functions in repairing alkylated DNA. We decided to focus our efforts on studying the repair of O^6-meG damage in a species that has only ATL protein and lacks Ogt protein.

T. thermophilus HB8 (TTHB8) is a Gram-negative bacterium that grows at temperatures above 75°C (*18*). It is the most thermophilic bacterium for which a gene manipulation system has been established (*19–21*). Proteins from this bacterium are stable against thermal denaturation and are suitable for physicochemical studies. We selected TTHB8 for the systematic study of the structure and function of all proteins from a single organism in a project named the 'Whole Cell Project' (*22*, *23*). We found only a single Ogt homologue, TTHA1564, in the TTHB8 genome. This gene is annotated as *ogt* and the corresponding amino acid sequence displays 34 and 37% identity (49 and 56% similarity) to AGT from *E. coli* and human, respectively. TTHA1564 is moderately homologous to normal Ogt and ATL proteins found in other species, including a similar DNA-binding domain. However, TTHA1564 does not have a cysteine residue in its putative active site and is therefore assumed to be an ATL protein. Interestingly, TTHA1564 is very similar to ATL protein from other species, but in this case the tryptophan residue at the putative active site is replaced by alanine (PAHR). Because ATL protein appears to be involved in repairing methylated DNA from *S. pombe*, we anticipated that TTHA1564 may play an analogous role in TTHB8.

In order to assess how TTHA1564 is involved in repairing alkylation damages of DNA, we describe here the biochemical characterization of TTHA1564. We initially examined phenotypes of TTHB8 *ttha1564*-deletion mutants, and overexpressed and purified TTHA1564 as a maltose-binding protein (MBP)-fusion. TTHA1564 displays no methyltransferase activity in the presence of O^6-meG-containing DNA. However, quantitative studies show that TTHA1564 binds to O^6-meG-containing DNA with higher affinity than normal (unmethylated) DNA. Furthermore, TTHA1564 binds to O^6-meG-containing DNA with nucleotide flipping. These results suggest TTHA1564 acts as a damage sensor that presents O^6-meG and possibly other O^6-alkylation lesions for processing by other repair pathways. Furthermore, our studies show that TTHA1564 can interact with nucleotide excision repair proteins and RNA polymerase.

MATERIALS AND METHODS

Materials—DNA-modifying enzymes, include restriction enzymes, were purchased from TakaraBio (Otsu, Japan). Yeast extract and polypeptone were from Difco (Detroit, MI, USA) and Nihon Pharmaceutical Co., Ltd (Tokyo, Japan), respectively. *Escherichia coli* strains DH5α and Rosetta (DE3) together with plasmids pT7Blue and pET-15b were from Novagen (Madison, WI, USA). The plasmid pGEX-5X-1pGEX was from GE Healthcare Biosciences (Piscataway, NJ, USA). Amylose resin and pMAL-cRI were from New England Biolabs (Beverly, MA, USA). TOYOPEARL-SuperQ, TOYOPEARL-Phenyl and TOYOPEARL-Ether 650M were from Tosoh (Tokyo, Japan). SensorChip CM5 and amine coupling kit were from Biacore AB (Uppsala, Sweden). The synthesized oligonucleotides used for the methyl group transfer assay and gel shift assay were from FASMAC (Atsugi, Japan). Other synthesized DNA oligomers were from BEX (Tokyo, Japan). Human MGMT (hMGMT) was from Sigma (St Louis, MO, USA). All other reagents used in this study were of the highest available commercial grade.

Construction of Expression Plasmids and Overexpression—Sequence data for TTHA1564, TTHA1440 and TTHA1323, corresponding to the *ttha1564*, *uvrA* and *mutL* genes, respectively, were obtained from the

TTHB8 genome project (DDBJ/EMBL/GeneBank AP008226). Using this information, six primers (i.e. forward and reverse) for amplification of the three target genes were designed and synthesized. The PCR was carried out using LA Taq polymerase with the appropriate pair of primers as follows: 5′-ATATCATATGTGG CTCCCCACGCCCTTAGGTCCCCT-3′ and 5′-ATATAGAT CTTTATTAAAGGGCCCCCTCAAAGCGGA-3′ (*ttha1564*), 5′-ATATCATATGGACCGCATCGTCATCCGG-3′ and 5′-ATATAGATCTTTATTAGTCCGCCGCCACCCCGAT-3′ (*uvrA*), and 5′-ATATCATATGATCCGCCCCCTCCCTCCG GAGCTTAG-3′ and 5′-ATATAGATCTTTATTAAGGTTCT CGGGGTAGAGGTG-3′ (*mutL*). Forward and reverse primers contained *Nde*I and *Bgl*II recognition sites (underlined), respectively. The amplified fragments of *ttha1564* and *mutL* were ligated into the pT7Blue by TA cloning. Sequence analysis revealed that the constructions were error-free. The gene fragments were then digested with *Nde*I and *Bgl*II and ligated into the compatible sites of pGEX-NdeI, in which an *Nde*I linker was inserted into the *Eco*RI site of pGEX-5X-1, creating pGEX/*ttha1564* and pGEX/*mutL*. The gene fragments of pGEX/*ttha1564* and pGEX/*mutL* were transferred into pMAL-cRI using *Eco*RI and *Sal*I sites, creating pMAL/*ttha1564* and pMAL/*mutL*. The gene fragment of *uvrA* was digested with *Nde*I and *Bgl*II and ligated into the compatible sites of pET-HisTEV, creating pET-HisTEV/*uvrA*. pET-HisTEV contains the tobacco etch virus (TEV) protease-recognition site, Glu-Asn-Leu-Tyr-Phe-Gln-Gly, instead of the thrombin-recognition site of the pET-15b vector (Novagen). *E. coli* DH5α cells transformed by pMAL/*ttha1564* or pMAL/*mutL* and *E. coli* Rosetta(DE3) cells transformed by pET-HisTEV/*urvA* plasmid were grown at 37°C for 20 h using 1.5 l of LB medium containing 50 μg/ml ampicillin. The cells were harvested by centrifugation and stored at −20°C.

Purification—All purification steps described below were carried out at room temperature. The method of purification of MBP-TTHA1564 and MBP-MutL was as follows. Frozen cells (5 g) were suspended in 50 ml of buffer I [50 mM Tris–HCl (pH 8.0), 1 mM EDTA, 1 mM 2-mercaptoethanol] and disrupted by ultrasonication on ice. The cell lysate was clarified by centrifugation at ~30,000*g* for 20 min and the supernatant was then applied to an Amylose Resin column (bed volume 15 ml) that had been equilibrated in buffer I. Proteins were eluted with a linear gradient of maltose from 0 to 10 mM in a total volume of 200 ml of buffer I. Fractions containing the MBP-TTHA1564 or MBP-MutL were pooled and applied to a TOYOPEARL-SuperQ column (bed volume 15 ml) previously equilibrated with buffer I. The proteins were eluted with a linear gradient of NaCl from 0 to 1.0 M in a total volume of 200 ml of buffer I. Solid ammonium sulphate was added to the fractions containing MBP-TTHA1564 or MBP-MutL protein to a final concentration of 1.0 M. The protein solution was then applied to a TOYOPEARL-Ether 650 M column (bed volume 10 ml) previously equilibrated with buffer I containing 1.0 M ammonium sulphate. Proteins were eluted with a linear gradient of ammonium sulphate from 1.0 to 0 M in a total volume of 150 ml of buffer I. Fractions containing the MBP-TTHA1564 or MBP-MutL were collected and pooled. The collected solution containing MBP-TTHA1564 was dialysed against buffer II [20 mM Tris–HCl (pH 8.0), 50 mM NaCl, 1 mM EDTA, 1 mM dithiothreitol (DTT), 5% (v/v) glycerol] at 4°C.

The method for the purification of His6-UvrA was as follows. Frozen cells (5 g) were suspended in 50 ml of buffer III [50 mM Tris–HCl (pH 8.0), 5 mM $ZnSO_4$] and disrupted by ultrasonication on ice. The cell lysate was incubated at 70°C for 10 min and then centrifuged at ~30,000*g* for 20 min. The clarified supernatant was applied to a His-Bind Resin column (bed volume 15 ml) that had been charged with buffer IV (100 mM $NiCl_2$) and equilibrated with buffer V [20 mM Tris–HCl (pH 8.0), 500 mM NaCl, 10% (v/v) glycerol, 10 mM imidazole]. Proteins were eluted with a linear gradient of imidazole from 10 to 500 mM in a total volume of 200 ml of buffer V. Solid ammonium sulphate was added to the fractions containing the His6-UvrA protein to a final concentration of 1.0 M. The protein solution was then applied to a TOYOPEARL-Phenyl column (bed volume 15 ml) previously equilibrated with buffer I containing 1.0 M ammonium sulphate. The proteins were eluted with a linear gradient of ammonium sulphate from 1.0 to 0 M in a total volume of 200 ml of buffer I. The collected solution containing His6-UvrA dialysed against buffer VI [50 mM Tris–HCl (pH 8.0)] at 4°C. The fractions containing His6-UvrA were applied to a TOYOPEARL-SuperQ column (bed volume 15 ml) previously equilibrated with buffer I. The proteins were eluted with a linear gradient of NaCl from 0 to 1.0 M in a total volume of 200 ml of buffer I. Fractions containing UvrA were collected. At each chromatography step, the purity was assessed by SDS–PAGE using a 10.5% (w/v) acrylamide gel. Purified MBP-TTHA1564, MBP-MutL and UvrA were identified by peptide mass fingerprinting with MALDI-TOF MS.

Methyltransferase Assay—Methyltransferase activity was assessed by demethylation analysis of DNA using methylation-specific restriction enzyme and by methylation analysis of the enzyme using mass spectrometry. A dsDNA duplex was made by annealing a 5′-^{32}P-labelled oligonucleotide 5′-GCCCGGCCAXCTGCAGTT-3′ (X = O^6-meG) to the complementary strand containing a cytosine opposite the O^6-meG. The melting temperature of this duplex was calculated to be about 70°C, which enabled us to perform the assay at 55°C. The duplex (10 nM) was incubated with 2.0 μM TTHA1564 in buffer II (10 μl) at 37°C for 16 h. After phenol/chloroform treatment followed by ethanol precipitation, the purified dsDNA was digested with *Pvu*II in 10 mM Tris–HCl (pH 7.5), 10 mM $MgCl_2$, 1 mM DTT and 50 mM NaCl at 37°C for 3 h. For demethylation analysis of product DNA, the reaction was stopped by addition of an equal volume of sample buffer (5 mM EDTA, 80% deionized formamide, 10 mM NaOH, 0.1% bromophenol blue, 0.1% xylene cyanol) and then the solution was loaded onto a 15% acrylamide gel (8 M urea and ×1 TBE buffer) and electrophoresed in ×1 TBE buffer. The gel was analysed as described earlier. A positive control experiment was carried out using hMGMT according to product information from Sigma, with minor modifications. For methylation analysis of the enzyme, the reactant was digested with Factor Xa in buffer II at 21°C for 16 h and then the

mixture was separated by SDS–PAGE. After staining the gel with Coomassie Brilliant Blue R-250, the band containing TTHA1564 was excised and in-gel digested with trypsin (Trypsin Gold; Promega, Madison, WI, USA). The peptide fragments were analysed by MALDI-TOF MS for identification of methylation.

Gel Shift Assay—Synthesized oligonucleotides (5′-GC CCGGCCAXCTGCAGTT-3′, X = O^6-meG or G) were labelled at the 5′ end with [γ-^{32}P]ATP using T4 polynucleotide kinase. Double-stranded DNA (dsDNA) substrates were made by annealing the labelled oligonucleotide to the complementary oligonucleotide containing a cytosine opposite the O^6-meG. DNA–protein complex was analysed by gel shift at room temperature (*24*). The reaction was carried out at room temperature in a 10 μl of buffer II containing 0–2.0 μM protein and 10 nM ^{32}P-labelled single-stranded DNA (ssDNA) or dsDNA. The mixtures were loaded onto a 12% (w/v) polyacrylamide gel and electrophoresed in ×1 TBE buffer (89 mM Tris–borate and 2 mM EDTA). The gel was dried and placed in contact with an imaging plate. The bands were visualized and analysed using a BAS2000 image analyzer (Fuji Film, Tokyo, Japan). Competitive gel shift assays were performed using the ^{32}P-labelled ssDNA and unlabelled ssDNA. In these reactions 2.0 μM TTHA1564 was incubated with 10 nM of ^{32}P-labelled ssDNA and 0–10 μM of unlabelled oligonucleotide in buffer II.

Fluorescence Analysis of Base Flipping—A synthesized oligonucleotide [5′-GGGTGTTGAXYTAGTTGTCAT-3′, where X = O^6-meG, Y = 2-aminopurine (2AP)] was annealed to a complementary oligonucleotide (5′-ATG ACAACTATCTCAACACCC-3′) to obtain fluorescent dsDNA. The 16 μM fluorescent dsDNA was incubated with 0–16 μM TTHA1564 in buffer II (200 μl). Fluorescence emission spectra of the mixture with an excitation wavelength of 315 nm were obtained at 25°C with a HITACHI spectrofluorometer, F-4500.

Deletion Disruption of the T. thermophilus tta1564 *Gene*—The *tta1564* gene deletion mutant was constructed according to the published recombination method (*21*). We constructed a plasmid containing the *tta1564* gene interrupted by a heat-stable kanamycin resistance gene, *htk* (*20*). *T. thermophilus* HB8 was transformed by this plasmid and three kanamycin-resistant clones were isolated as disruptants of the *tta1564* gene. Deletion of the *tta1564* gene on the chromosomal DNA was subsequently verified by PCR analysis using genomic DNA as template.

Measurement of Streptomycin Resistance—Overnight cultures of *T. thermophilus* HB8 WT, Δ*tta1564* and Δ*mutS* [a gift from Dr Kenji Fukui (RIKEN SPring-8 Center)] strains were plated on TT-streptomycin plates [4% (w/v) polypeptone, 2% (w/v) yeast extract, 1% (w/v) NaCl, 15% (w/v) phytagel and 50 μg/ml streptomycin (pH 7.5)] and then incubated at 70°C for 24 h. The number of colonies of streptomycin-resistant mutants on each plate was counted. Overnight cultures were also diluted 10^8-fold into TT medium [8% (w/v) polypeptone, 4% (w/v) yeast extract, 3% (w/v) NaCl, 400 μM $MgCl_2$, 400 μM $CaCl_2$ (pH 7.4)] and the diluted cultures were plated on TT plates [4% (w/v) polypeptone, 2% (w/v) yeast extract, 1% (w/v) NaCl, 15% (w/v) phytagel (pH 7.5)] and incubated at 70°C for 24 h. The number of colonies on each plate was then counted. The mutation rate was established as the ratio between the number of colonies growing on medium containing streptomycin and the total number of cells plated (*25*).

Pull Down Assay—About 300 nmol of MBP-TTHA1564 or MBP-MutL in buffer VII [20 mM Tris–HCl (pH 8.0), 50 mM NaCl] was applied to an amylose resin column (bed volume 2 ml) that had been equilibrated with buffer VI. Frozen TTHB8 cells (0.8 g) were suspended in 8 ml of buffer VI and disrupted by ultrasonication on ice. Next, the lysate was centrifuged at ~30,000*g* for 20 min. Then, 7 ml of the supernatant was applied to the MBP-TTHA1564-immobilized or MBP-MutL-immobilized column. After thoroughly washing the column with buffer VI, bound proteins were eluted with 6 ml of buffer VI containing 10 mM maltose. The proteins in the eluate were separated by SDS–PAGE, and identified by peptide mass fingerprinting using MALDI-TOF MS. For analysis of interaction of TTHA1564 with UvrA, 46 nmol of purified UvrA in buffer VII was applied to the MBP-TTHA1564-immobilized column.

Surface Plasmon Resonance Assay—A surface plasmon resonance assay was performed using a BIAcore 1000 instrument. Purified recombinant MBP-TTHA1564 and MBP (at a concentration of 0.85 μM) were immobilized onto the Sensor Chip CM5 using amine coupling. The immobilization resulted in 950 and 200 resonance units for MBP-TTHA1564 and MBP, respectively. All successive experiments were performed at 25°C in buffer VII as the running buffer. UvrA (10 μl) was injected at a flow rate of 10 μl/min at concentrations ranging from 100 to 800 nM. Bound proteins were then dissociated by injection of 1 M NaCl. The MBP-immobilized flow cell was used as a reference to subtract nonspecific binding and baseline drift. Based on the reference-subtracted sensorgram data, dissociation constants (K_d) were determined by global fitting to a 1 : 1 Langmuir model using the BIAevaluation 3.0 software.

RESULTS

TTHA1564 Lacked Methyltransferase Activity to O^6-meG in DNA—We examined the methyltransferase activity of TTHA1564 by demethylation analysis of O^6-meG-containing DNA substrate (Fig. 2A). Reactions were performed at 37 or 55°C because MBP fused to TTHA1564 was unstable above 55°C. The DNA substrate included a *Pvu*II recognition sequence (5′-CAGCTG-3′) containing O^6-meG at the third base position (underlined). Thus, the methylation status of the substrate could be conveniently determined by incubation with the methylation-sensitive restriction enzyme *Pvu*II. DNA pretreated with TTHA1564 was not susceptible to cleavage by *Pvu*II (Fig. 2A), suggesting TTHA1564 lacks methyltransferase activity under the conditions used in our experiments. This analysis was validated by a positive control experiment, in which the same DNA substrate pretreated with hMGMT was cleaved by *Pvu*II (Fig. 2B). Despite the fact that Ogt requires no cofactor, we could not exclude the possibility that TTHA1564 might need a cofactor for activity. Therefore, we also

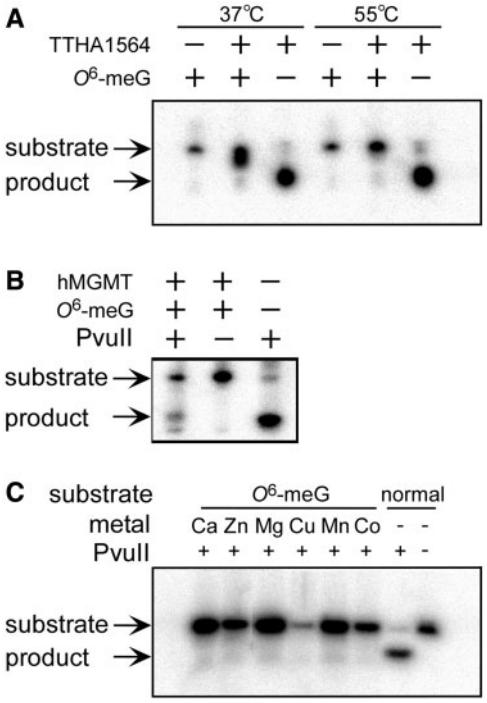

Fig. 2. **Methyltransferase activity assay of TTHA1564 by demethylation analysis.** (A) The activity of TTHA1564 (2 μM) for 18 bp dsDNA (10 nM). The product DNA was incubated with *Pvu*II and then analysed by polyacrylamide gel electrophoresis. In the *O^6-meG* row, dsDNA containing O^6-meG within the recognition sequence of *Pvu*II is indicated by the plus sign, whereas the normal dsDNA by the minus sign. (B) The positive control experiment using hMGMT. The middle lane represents the sample not treated with *Pvu*II. (C) Activity in the presence of metal ions at 10 mM. In the *normal* lanes, the assays were performed for normal dsDNA in the presence of TTHA1564, and the right lane represents the sample not treated with *Pvu*II.

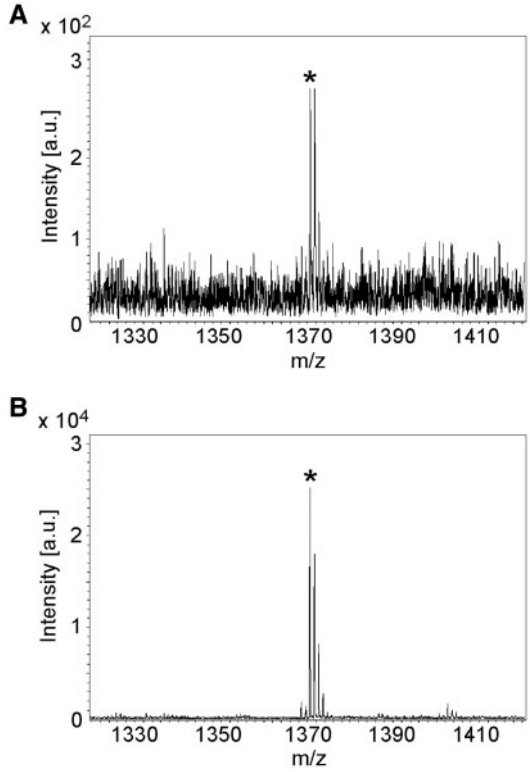

Fig. 3. **Methylation assay of TTHA1564 by mass spectrometry.** After incubation with normal dsDNA (A) or O^6-meG-containing dsDNA (B), the protein was subjected to SDS–PAGE. The excised band was in-gel digested with trypsin and the fragments were analysed by MALDI-TOF MS. The peak marked with an asterisk (m/z of 1369.6) corresponds to the fragment containing the unique cysteine residue and putative active site motif.

performed the same experiments in the presence of metal ions (Fig. 2C), but no demethylation of the substrate DNA could be detected.

We reasoned that if a methyl group is transferred from O^6-meG-containing DNA to TTHA1564, the mass of the protein will increase by 14 Da. Thus, we carried out mass spectrometric analysis to examine the possible transfer of a methyl group to the protein. Tryptic fragments of TTHA1564 incubated with O^6-meG-containing DNA were analysed by MALDI-TOF MS. TTHA1564 has a unique cysteine residue located just N-terminal to the putative active site. A single tryptic fragment (108-ACPFFLLVPAHR-119) contains both the cysteine residue and the putative active site motif. As anticipated, analysis of TTHA1564 prior to incubation with O^6-meG-containing DNA gave a peak with an m/z of 1369.6 (Fig. 3A), which corresponded to the theoretical mass of the Cys-containing fragment without modification. However, after incubation of the protein with O^6-meG-containing DNA we also identified a peak with an m/z of 1369.6. No peak corresponding to the Cys-containing fragment with a mass increase of 14 could be detected (Fig. 3B). Furthermore, none of the other tryptic fragments identified in this analysis showed an increase in mass over the anticipated values based on the primary amino acid sequence of the protein (data not shown). Thus, our results indicate that TTHA1564 alone does not possess methyltransferase activity under the experimental conditions used in this study.

TTHA1564 Specifically Binds to O^6-meG-containing DNA—To examine DNA-binding activity of TTHA1564, gel shift assays were performed using four kinds of 18-mer or 18-bp DNA: O^6-meG-containing ssDNA, O^6-meG-containing dsDNA, normal ssDNA and normal dsDNA (Fig. 4). In each case, a complex of the protein with the respective DNA species was detected. Plots showing the percentage of shifted band versus protein concentration for both ssDNA and dsDNA are given in Fig. 4B. Interestingly, O^6-meG-containing DNA showed a larger percentage of shifted bands compared to normal DNA. However, this result was insufficient to demonstrate whether TTHA1564 has specificity towards O^6-meG-containing DNA.

To further investigate whether TTHA1564 has a higher affinity for O^6-meG-containing DNA over normal DNA we carried out competitive inhibition assays. The competitive inhibition experiments were performed by incubating TTHA1564 with ^{32}P-labelled normal dsDNA and a varying concentration of cold competitor DNAs (Fig. 5A). Our results indicate that TTHA1564 specifically binds to O^6-meG-containing DNA in preference to

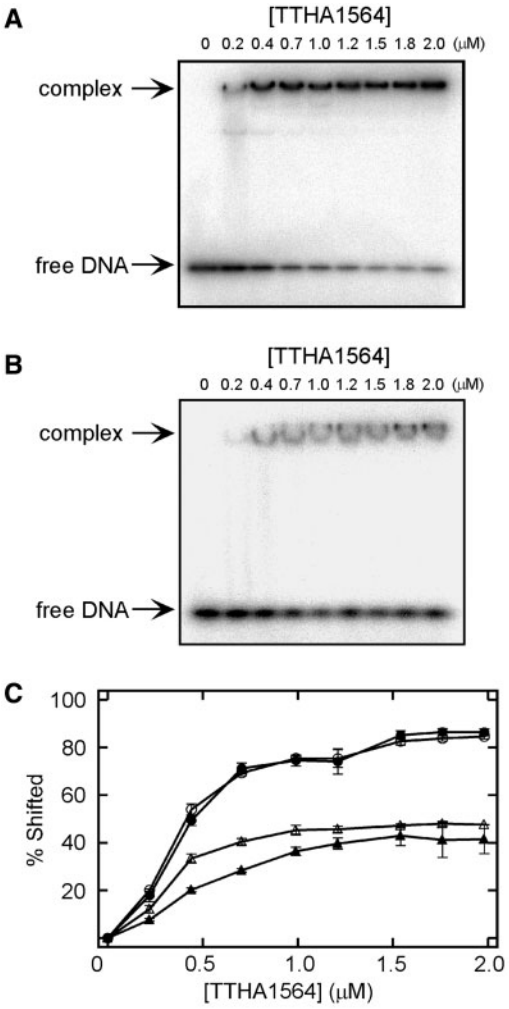

Fig. 4. **Gel shift assay of TTHA1564.** (A) TTHA1564 at the indicated concentration was incubated with 10 nM dsDNA (18 bp) containing O^6-meG. (B) TTHA1564 at the indicated concentration was incubated with 10 nM ssDNA (18-mer) containing O^6-meG. (C) The percentages of complexed substrate plotted against protein concentration. Symbols represent the following: filled circles, O^6-meG-containing ssDNA; open circles, O^6-meG-containing dsDNA; filled triangles, normal ssDNA and open triangles, normal dsDNA.

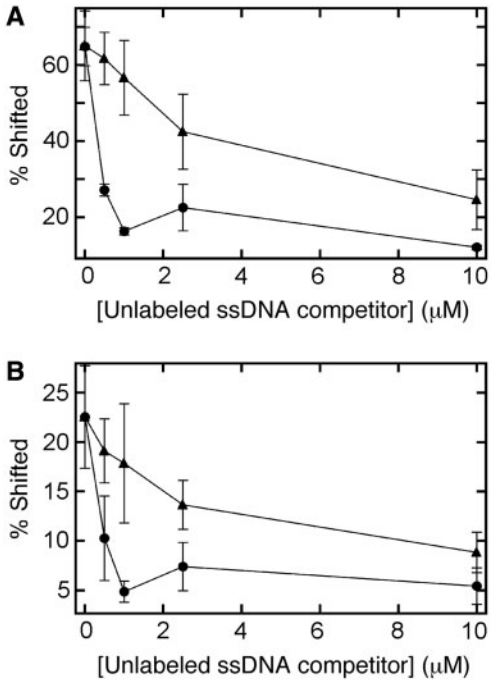

Fig. 5. **Competitive gel shift assay.** (A) Inhibition of ^{32}P-labelled O^6-meG-containing ssDNA-TTHA1564 complex with unlabelled ssDNA competitors. (B) Inhibition of ^{32}P-labelled normal ssDNA-TTHA1564 complex with unlabelled ssDNA competitors. TTHA1564 (2.0 μM) was incubated with 10 nM of ^{32}P-labelled ssDNA (18-mer) and 0–10 μM of unlabelled ssDNA (18-mer) at room temperature. Unlabelled ssDNA competitors were O^6-meG-containing ssDNA (circles) and normal ssDNA (triangles) in both panels. The percentages of complexed substrate plotted against concentration of unlabelled ssDNA competitors.

normal DNA. Similar results were obtained in the same experiment with ^{32}P-labelled O^6-meG-containing DNA (Fig. 5B). From these competition studies, K_d values of TTHA1564 with normal DNA or O^6-meG-containing DNA were estimated to be 3.7 and 0.41 μM, respectively. Our results indicate that TTHA1564 exhibits a ~9-fold greater affinity for DNA containing O^6-meG compared with normal DNA.

TTHA1564 Flips O^6-meG Nucleotides from DNA—To elucidate the mechanism of recognition of O^6-meG in DNA, we investigated base flipping using fluorescence dsDNA. 2AP, a fluorescent analogue of adenine, has often been used as a probe to detect base flipping (*26*). In this experiment, one DNA strand contains a 2AP residue 3′ adjacent to O^6-meG residue. When 2AP is situated inside the duplex, its fluorescence is quenched by interaction with the neighbouring bases. However, when the base adjacent to 2AP flips out from the duplex there is an increase in fluorescence intensity.

Upon addition of TTHA1564, the 2AP-containing dsDNA showed a significant change in the fluorescence spectrum with a peak at around 366 nm (Fig. 6A). Furthermore, the fluorescence intensity increases in a protein concentration-dependent manner (Fig. 6B). A similar spectral change of the same fluorescent dsDNA was also observed for *Methanocaldococcus jannaschii* Ogt (MJOgt) (Fig. 6C and D). MJOgt possesses a cysteine residue in its active site and exhibits methyltransferase activity (*27*). These results suggest a flipping-out of O^6-meG from the duplex upon binding of protein. Therefore, it can be assumed that TTHA1564 rotates the O^6-meG base moiety around the DNA backbone into an extrahelical position and recognizes the base in the putative active site. Therefore, we conclude that TTHA1564 has the same mechanism of recognition of O^6-meG base as those of other Ogt proteins containing a PCHR active site, although THA1564 has no cysteine residue in its active site.

Disruption of ttha1564 *Gene Increases the Spontaneous Mutation Rate*—To investigate the physiological role of TTHA1564 *in vivo*, we made a *ttha1564*-disruptant mutant (Δ*ttha1564*). The Δ*ttha1564* and WT strains exhibited similar growth rates in rich medium (data not shown). We also measured the spontaneous mutation

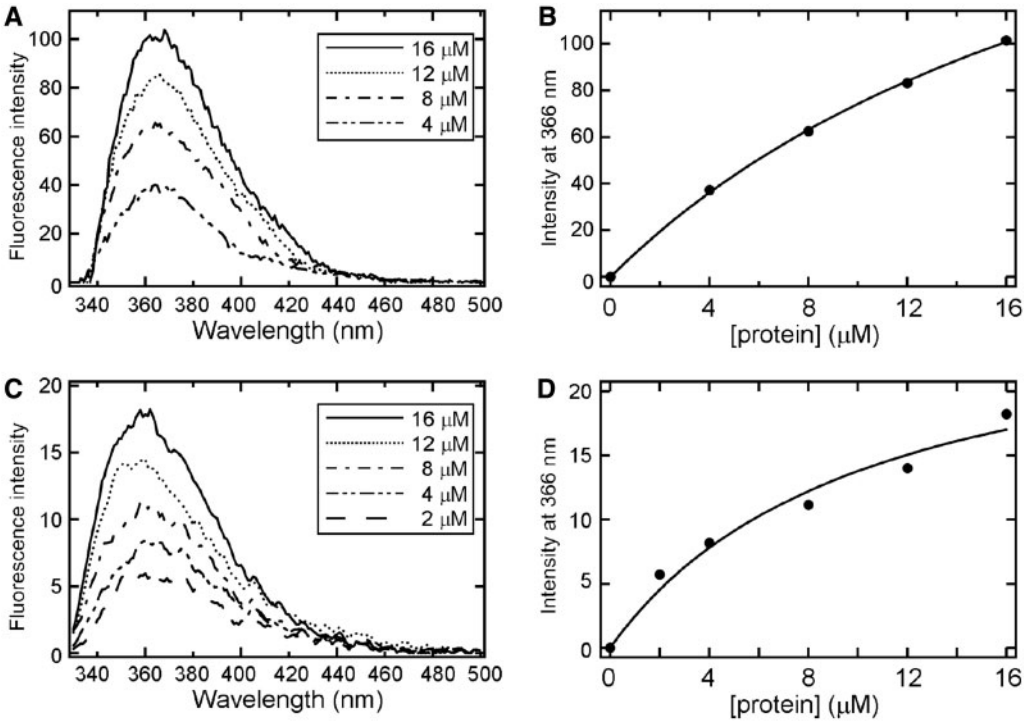

Fig. 6. **Fluorescence analysis of base flipping by TTHA1564.** The 2-AP and O^6-meG-containing dsDNA (16 μM) was incubated with TTHA1564 (A) or MJOgt (C). We measured fluorescence spectra of the mixture using an excitation wavelength of 315 nm. The spectra shown were obtained by subtracting the spectrum in the absence of TTHA1564 from those in the presence of TTHA1564. Fluorescence intensities at 366 nM were plotted against protein concentrations of TTHA1564 (B) or MJOgt (D).

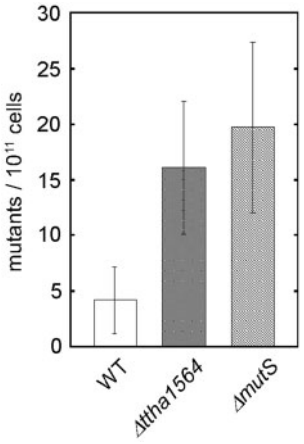

Fig. 7. **Effect of disruption of the *ttha1564* gene on the spontaneous mutation rate.** Spontaneous mutation rates for WT, Δ*ttha1564* and Δ*mutS* strains were measured by monitoring streptomycin resistance. The mutation rate was calculated as the ratio between the number of colonies on the medium with streptomycin and the total number of cells plated.

rate of the WT and Δ*ttha1564* strains using streptomycin resistance as a phenotypic marker (Fig. 7) (*25*). The mutation rate of Δ*ttha1564* was significantly higher than WT (significant level, $P < 9 \times 10^{-12}$). This mutation rate was comparable to that of *mutS*-disruptant strain (Δ*mutS*) of TTHB8. Because MutS is a mismatch repair protein, these results strongly suggest that TTHA1564 is also involved in DNA repair *in vivo*.

TTHA1564 Interacts with a Nucleotide Excision Repair Protein—If TTHA1564 can recognize an O^6-meG lesion but cannot remove it from the DNA, it is reasonable to suppose that a known repair system may be involved in the repair of this lesion. To investigate a putative TTHA1564-related repair pathway, we attempted to identify proteins that interact with TTHA1564 using a pull-down assay involving a MBP-TTHA1564-immobilized column. Excluding MBP-TTHA1564, our pull-down assay detected approximately 40 bands in the fraction eluted from the MBP-TTHA1564-immobilized column with maltose (Fig. 8A). Furthermore, these protein bands were not detected in the fraction eluted from the MBP-immobilized column (Fig. 8A). Therefore, the 40 protein species appear to specifically interact with TTHA1564. Peptide mass fingerprinting by MALDI-TOF MS successfully identified 21 out of the 40 candidate TTHA1564-binding proteins (Table 1).

Many DNA-binding proteins were identified, among which UvrA (TTHA1440), a nucleotide excision repair (NER) protein, was the most intriguing. UvrD helicase (TTHA1427) was also identified, although the number of matched peptides was not significant. DNA ligase [NAD^+] (TTHA1097) and UvrD helicase are known to be involved in DNA repair, including the NER pathway. It is also noteworthy that three subunits of RNA polymerase core enzyme, RpoA (TTHA1664), RpoB (TTHA1812) and RpoC (TTHA1813), appear to bind to TTHA1564. Our results also indicate that PIWI motif protein (TTHB068), putative Rad52 homologue (TTHA0081), as well as some additional proteins, may interact with TTHA1564.

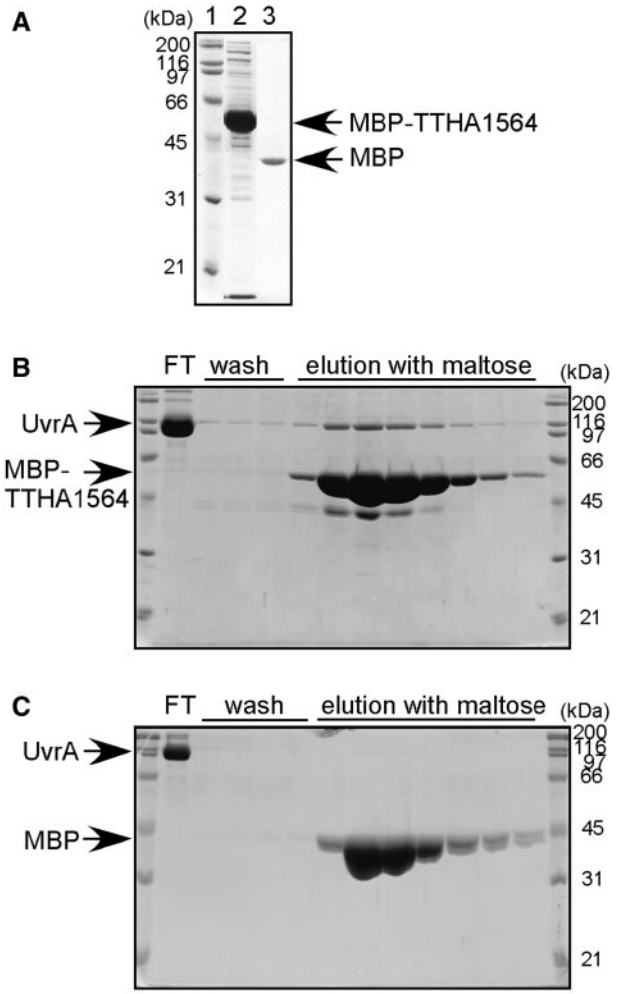

Fig. 8. **Identification of proteins interacting with TTHA1564.** (A) Pull-down assay using MBP-TTHA1564. Lane 1, protein size marker; lane 2, fraction eluted from the MBP-TTHA1564-immobilized column with maltose; lane 3, fraction eluted from the MBP-immobilized column with maltose. (B) Interaction of UvrA with TTHA1564. The purified UvrA was applied to a MBP-TTHA1564-immobilized column. Fractions from the flow-through (FT), eluted by washing with a buffer (wash) and eluted with maltose (elution with maltose) were analysed by SDS–PAGE. The series of bands just under the MBP-TTHA1564 correspond to MBP, probably generated by adventitious degradation of. MBP-TTHA1564. (C) Interaction of UvrA with MBP (control experiment).

It is possible that the apparent interaction between TTHA1564 and the other DNA-binding proteins identified in this study could be an artifact of their interaction with the same fragment of DNA. To verify that TTHA1564 directly interacts with these candidate proteins, we carried out a control experiment using a MBP-fused form of *T. thermophilus* MutL. MBP-MutL was a convenient control in these experiments because MutL is also a DNA-binding protein. Thus, we overexpressed MutL as a MBP fusion. Several proteins that interacted with MBP-MutL were identified (Table 2), but none of the significantly interacting proteins are listed in Table 1. Note that DNA-binding protein HU, a cold shock protein and the α subunit of RNA polymerase appear in both Tables, but their respective scores were not significant in either experiment. We cannot exclude the possibility that MutL interacts with RNA polymerase, although the subsequent control experiments support the hypothesis that the interaction of TTHA1564 with UvrA and RNA polymerase is meaningful. We can, however, conclude that RNA polymerase binds TTHA1564 more tightly than MutL.

Next, we focused on the interaction of TTHA1564 with UvrA. To verify whether TTHA1564 protein interacts with UvrA, we carried out the same assay using purified UvrA instead of the crude protein extract from TTHB8 cells. UvrA was eluted in the flow-through fraction and in the TTHA1564-eluted fraction (Fig. 8B). Thus, at least a proportion of the UvrA applied to the column appears to interact with TTHA1564. In a control experiment using an MBP-immobilized column, UvrA eluted exclusively in the flow-through fraction (Fig. 8C). This experiment indicates that UvrA does not interact with the column resin or with MBP. Taken together, our experiments indicate that the interaction of MBP-TTHA1564 with UvrA is significant.

To further investigate TTHA1564-UvrA interaction in detail, we carried out surface plasmon resonance assays. Our results verify that UvrA interacts with TTHA1564 immobilized on a sensor chip (Fig. 9). The association rate constant of TTHA1564 for UvrA is $107\,mM^{-1}s^{-1}$, and the dissociation rate constant is $3.3 \times 10^{-3}\,s^{-1}$. The dissociation constant K_d is 30 nM at 25°C.

DISCUSSION

TTHA1564 is homologous to Ogt from other species but lacks a critical cysteine residue in its putative active site. In this study, we have used a variety of methods to investigate whether TTHA1564 is involved in repairing alkylation damaged DNA. As anticipated, given the lack of a cysteine residue in the active site, we were unable to detect any methyltransferase activity using our purified TTHA1564. Unfortunately, we were unable to carry out our experiments at temperatures above 55°C due to instability of the MBP portion of the recombinant protein. Therefore, we cannot entirely exclude the possibility that TTHA1564 exhibits methyltransferase activity above 70°C, which is the optimal growth temperature for TTHB8. Nevertheless, we conclude that TTHA1564 is an ATL protein based on sequence analysis and on our biochemical characterization studies.

We also assessed the DNA-binding activity of TTHA1564. Gel shift assays confirmed that TTHA1564 binds to DNA. Furthermore, TTHA1564 binds to O^6-meG-containing DNA with a significantly higher affinity (about 9-fold) than to normal DNA. This is the first report of quantitative measurements related to the affinity of an ATL protein for O^6-meG-containing DNA. The K_d value (0.41 μM) of TTHA1564 to O^6-meG-containing DNA is similar to that of MGMT (0.5–20 μM) (*14*, *28–31*).

We also observed the flipping-out of O^6-meG base upon binding TTHA1564. Base flipping involves rotation of backbone bonds in dsDNA to locate a nucleotide inside the protein pocket, and is a mechanistic feature common to most DNA glycosylases and methyltransferases (*32*).

Table 1. **Summary of proteins interacted with TTHA1564.**

Gene number	Gene ID	Protein name	Molecular mass (kDa)	Peptides matched
TTHA1812	YP_145078	RNA polymerase β′ chain (RpoC)	170.7	29
TTHA1813	YP_145079	RNA polymerase β chain (RpoB)	125.2	20
TTHA1440	YP_144706	Excinuclease ABC subunit A (UvrA)	105.1	10
TTHA1355	YP_144621	DNA gyrase subunit A	89.1	8
TTHA1139	YP_144405	Polynucleotide phosphorylase	78.1	17
TTHA1097	YP_144363	DNA ligase [NAD^+]	76.9	9
TTHB068	YP_145307	Hypothetical protein	76.6	10
TTHA1634	YP_144900	Peptide ABC transporter, peptide-binding protein	70.4	9
TTHA1329	YP_144595	Glutamine synthetase	50.5	14
TTHA0196	YP_143462	Transporter, periplasmic component	40.3	5
TTHA1664	YP_144930	DNA-directed RNA polymerase α chain (RpoA)	35.0	6
TTHB045	YP_145284	Repeat motif-containing protein	31.9	5
TTHA0244	YP_143510	Single-stranded DNA-binding protein (SSB)	29.8	8
TTHA0081	YP_143347	Conserved hypothetical protein	24.3	4
TTHA1657	YP_144923	AT-rich DNA-binding protein	23.2	6
TTHA0175	YP_143441	Cold shock protein	8.2	4
Proteins below were not significant.				
TTHA0506	YP_143772	Malate synthase	58.7	7
TTHA1427	YP_144693	UvrD helicase	57.4	7
TTHA1153	YP_144419	Mercuric reductase	48.5	4
TTHA0718	YP_143984	Uracil-DNA glycosylase A (UDGA)	23.0	5
TTHA1349	YP_144615	DNA-binding protein HU	10.4	3

These proteins were identified by peptide mass fingerprinting with MALDI-TOF MS.

Table 2. **Summary of proteins interacted with MutL.**

Gene number	Gene ID	Protein name	Molecular mass (kDa)	Peptides matched
TTHA1261	YP_144527	4-α-glucanotransferase (amylomaltase)	57.2	14
TTHA0617	YP_143883	Nicotinate phosphoribosyltransferase	56.4	9
TTHA1542	YP_144808	Probable cell cycle protein MesJ	56.3	14
TTHA1213	YP_144479	Acetolactate synthase large subunit	55.7	7
TTHA0495	YP_143761	2-phosphoglycerate kinase	54.0	8
TTHA1563	YP_144829	(neo)pullulanase	53.7	10
TTHA0648	YP_143914	Probable glycosyltransferase	41.2	11
TTHA0196	YP_143462	Transporter periplasmic component	40.3	7
TTHA0645	YP_143911	Putative glycosyltransferase	37.9	6
TTHA1689	YP_144955	50S ribosomal protein L2	30.5	7
TTHA1692	YP_144958	50S ribosomal protein L3	22.4	5
TTHA1680	YP_144946	50S ribosomal protein L5	21.0	5
TTHA1677	YP_144943	50S ribosomal protein L6	19.5	8
TTHA0255	YP_143521	Ferric uptake regulation protein	17.0	4
TTHA1349	YP_144615	DNA-binding protein HU	10.4	4
Proteins below were not significant.				
TTHA1328	YP_144594	5′-nucleotidase precursor	55.5	5
TTHB198	YP_145437	Hypothetical protein	45.0	6
TTHA0579	YP_143845	Sugar ABC transportor ATP-binding protein	42.1	6
TTHA1064	YP_144330	Diaminohydroxyphosphoriboxylaminopyrimidine deaminase + 5-amino-6-(5-phosphoribosylamino) uracil reductase (RibD)	40.7	5
TTHA1664	YP_144930	DNA-directed RNA polymerase α chain	35.0	4
TTHA0175	YP_143441	Cold shock protein	8.2	3

These proteins were identified by peptide mass finger printing with MALDI-TOF MS.

In the crystal structure of human AGT in complex with O^6-meG-containing dsDNA, the O^6-meG is flipped out from the base stack (*13*). These results suggest that TTHA1564 recognizes an O^6-meG base moiety by flipping of the target base out of the duplex in a similar manner to other Ogts. In hAGT, Tyr114 and Arg128 are involved in the nucleotide flipping. Corresponding tyrosine residues are also conserved in MJOgt (Tyr99 and Arg111) and TTHA1564 (Tyr88 and Arg100; Fig. 1). Therefore, we conclude that ATL proteins, including TTHA1564,

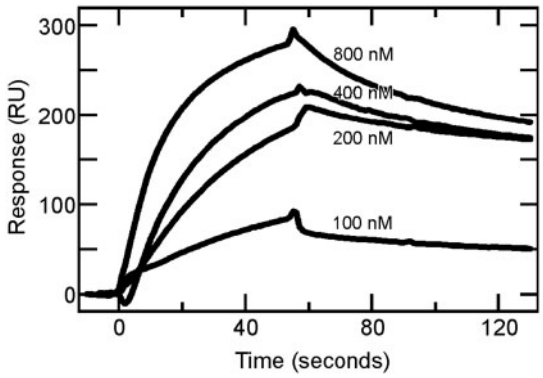

Fig. 9. **Surface plasmon resonance assay for interaction of TTHA1564 with UvrA.** The UvrA solution (100–800 nM) was injected over a sensor chip containing immobilized MBP-TTHA1564. The control sensorgrams for the sensor chip containing immobilized MBP were subtracted from the measuring sensorgrams.

possess all the necessary residues for flipping out O^6-meG, but lack the active site residues required for alkyltransferase activity.

We analysed the effect of disruption of the TTHA1564 gene on the growth rate and spontaneous mutation rate of TTHB8. No significant difference in the growth rate of WT strain and *ttha1564*-disruptant could be detected in rich media. However, the disruptant displayed a significantly increased spontaneous mutation rate, comparable to that of the *mutS* gene disruptant. These results strongly suggest that TTHA1564 is involved in DNA repair. Furthermore, the presence of a methylating agent caused 5- to 8-fold increase in spontaneous mutation frequency in the *ttha1564*-disruptant compared with the wild-type (personal communication). Since this experiment used His^+ reversion by G:C to A:T transition, this result suggest that TTHA1564 played an important role to prevent GC-to-AT transition mutations, which can be caused by O^6-meG mispairing with thymine (*2–4*).

Intriguingly, our results demonstrate that TTHA1564, despite lacking any detectable methyltransferase activity, is involved in repairing damage to DNA induced by O^6-meG. We hypothesized that TTHA1564 might be involved in repairing O^6-meG and possibly other O^6-alkylation lesions by acting as a damage sensor for a separate repair system. To examine whether TTHA1564 interacts with other proteins, we performed a pull-down assay. Our results show that TTHA1564 interacts with several proteins including UvrA and RNA polymerase. Interaction of TTHA1564 with UvrA was further confirmed using recombinant UvrA. The K_d value for interaction between UvrA and TTHA1564 strongly suggests this interaction is significant. In NER, UvrA acts as a damage recognition protein together with UvrB. NER can remove a wide range of DNA lesions that differ in terms of their chemistry and structure. It is known that O^6-meG is a substrate for NER in *E. coli*, although distortion of the DNA structure caused by this lesion is minimal (*33*, *34*). Therefore, TTHA1564 appears to recruit UvrA to the site of the O^6-meG lesion in order to efficiently initiate NER. Interestingly, it was suggested that the C145A mutant hAGT binds to O^6-methylguanine lesions in DNA and prevents their repair by NER (*35*). In the case of TTHA1564, interaction with UvrA may stimulate release of TTHA1564 from the DNA.

Our pull-down assay also identified the α, β, and β′ subunits of RNA polymerase as interacting with TTHA1564. Thus, we consider that RNA polymerase core enzyme interacts with TTHA1564. This finding prompted us to examine the functional association of TTHA1564 with the transcription-coupled repair pathway. The transcription-coupled repair pathway is triggered by an elongating RNA polymerase that becomes stalled at lesions in the DNA template and removes the stalled RNA polymerase from DNA and recruits UvrA to the lesion. Transcription-repair coupling factor (TRCF) removes a stalled RNA polymerase covering the damaged DNA and recruits UvrA (*36*, *37*). TRCF interacts with both RNA polymerase and UvrA (*38*). Our observation that TTHA1564 interacts with both UvrA and RNA polymerase raises the possibility that TTHA1564 may act like TRCF. Indeed, the binding affinity of TTHB8 UvrA for TTHB8 TRCF is similar to that of TTHA1564 (data not shown). In addition, the amino acid sequence of TTHA1564 shows some similarity to that of the β domain of TRCR and UvrB of TTHB8, which is an interaction domain to UvrA. However, there is currently no direct experimental evidence to support the notion that TTHA1564 may act like TRCF. Alternatively, it has been suggested that the transcription machinery may play an important role in sensing DNA damage and activating DNA repair pathways when stalled at blocking lesions (*39*). It is known that *E. coli* RNA polymerase efficiently bypasses O^6-meG lesions to insert uracil into the transcript opposite to O^6-meG, resulting in a C-to-U transition mutation (*40*). TTHA1564 bound to an O^6-meG lesion may prompt the RNA polymerase to stall at the lesion site. Involvement of TTHA1564 in NER, transcription-coupled repair and transcription remains to be examined.

This work was supported in part by Grant-in-Aid for Scientific Research 17770089 (to N.N.) from the Ministry of Education, Science, Sports and Culture of Japan.

We thank Dr Kwang Kim for his help in peptide mass fingerprinting. We also thank Professor Hisao Masukata for his help in surface plasmon resonance assays, and Drs Satoru Watanabe and Ryoichi Arai for providing us the pET-HisTEV vector. We are also grateful to Dr Toshihiro Ohta for providing us with information about the *ttha1564* disruptant before publication.

REFERENCES

1. Lindahl, T. and Wood, R.D. (1999) Quality control by DNA repair. *Science* **286**, 1897–1905
2. Loveless, A. (1969) Possible relevance of O-6 alkylation of deoxyguanosine to the mutagenicity and carcinogenicity of nitrosamines and nitrosamides. *Nature* **223**, 206–207
3. Snow, E.T., Foote, R.S., and Mitra, S. (1984) Base-pairing properties of O^6-methylguanine in template DNA during in vitro DNA replication. *J. Biol. Chem.* **259**, 8095–8100
4. Loechler, E.L., Green, C.L., and Essigmann, J.M. (1984) In vivo mutagenesis by O^6-methylguanine built into

a unique site in a viral genome. *Proc. Natl. Acad. Sci. USA* **81**, 6271–6275
5. Brent, T.P., Houghton, P.J., and Houghton, J.A. (1985) O^6-Alkylguanine-DNA alkyltransferase activity correlates with the therapeutic response of human rhabdomyosarcoma xenografts to 1-(2-chloroethyl)-3-(trans-4-methylcyclohexyl)-1-nitrosourea. *Proc. Natl. Acad. Sci. USA* **82**, 2985–2989
6. Mitra, S. and Kaina, B. (1993) Regulation of repair of alkylation damage in mammalian genomes. *Prog. Nucleic Acid Res. Mol. Biol.* **44**, 109–142
7. Olsson, M. and Lidahl, T. (1980) Repair of alkylated DNA in *Escherichia coli*. Methyl group transfer from O^6-methylguanine to a protein cysteine residue. *J. Biol. Chem.* **255**, 10569–10571
8. Lindahl, T., Demple, B., and Robins, P. (1982) Suicide inactivation of the *E. coli* O^6-methylguanine-DNA methyltransferase. *EMBO J.* **1**, 1359–1363
9. Wiestler, O., Kleihues, P., and Pegg, A.E. (1984) O^6-alkylguanine-DNA alkyltransferase activity in human brain and brain tumors. *Carcinogenesis* **5**, 121–124
10. Demple, B., Jacobson, A., Olsson, M., Robins, P., and Lindahl, T. (1982) Repair of alkylated DNA in Escherichia coli. Physical properties of O^6-methylguanine-DNA methyltransferase. *J. Biol. Chem.* **257**, 13776–13780
11. Boulden, A.M., Foote, R.S., Flemming, G.S., and Mitra, S. (1987) Purification and some properties of human DNA-O^6-methylguanine methyltransferase. *J. Biosci.* **11**, 215–224
12. Bhattacharyya, D., Foote, R.S., Boulden, A.M., and Mitra, S. (1990) Physicochemical studies of human O^6-methylguanine-DNA methyltransferase. *Eur. J. Biochem.* **193**, 337–343
13. Daniels, D.S., Woo, T.T., Luu, K.X., Noll, D.M., Clarke, N.D., Pegg, A.E., and Tainer, J.A. (2004) DNA binding and nucleotide flipping by the human DNA repair protein AGT. *Nat. Struct. Mol. Biol.* **11**, 714–720
14. Daniels, D.S. and Tainer, J.A. (2000) Conserved structural motifs governing the stoichiometric repair of alkylated DNA by O^6-alkylguanine-DNA alkyltransferase. *Mutat. Res.* **460**, 151–163
15. Pearson, S.J., Ferguson, J., Santibanez-Koref, M.F., and Margison, G.P. (2005) Inhibition of O^6-methylguanine-DNA methyltransferase by an alkyltransferase-like protein from *Escherichia coli*. *Nucleic Acids Res.* **33**, 3837–3844
16. Pearson, S.J., Wharton, S., Watson, A.J., Begum, G., Butt, A., Glynn, N., Williams, D.M., Shibata, T., Santibáñez-Koref, M.F., and Margison, G.P. (2006) A novel DNA damage recognition protein in *Schizosaccharomyces pombe*. *Nucleic Acids Res.* **34**, 2347–2354
17. Margison, G.P., Butt, A., Pearson, S.J., Wharton, S., Watson, A.J., Marriott, A., Caetano, C.M., Hollins, J.J., Rukazenkova, N., Begum, G., and Santibáñez-Koref, M.F. (2007) Alkyltransferase-like proteins. *DNA Repair (Amst.)* **6**, 1222–1228
18. Oshima, T. and Imahori, K. (1974) Description of *Thermus thermophilus* (Yoshida and Oshima) comb. nov. A non-sporulating thermophilic bacterium from a japanese thermal spa. *Int. J. Syst. Bacteriol.* **24**, 102–112
19. Yamagishi, A., Tanimoto, T., Suzuki, T., and Oshima, T. (1996) Pyrimidine biosynthesis genes (pyrE and pyrF) of an extreme thermophile, *Thermus thermophilus*. *Appl. Environ. Microbiol.* **62**, 2191–2194
20. Hoseki, J., Yano, T., Koyama, Y., Kuramitsu, S., and Kagamiyama, H. (1999) Directed evolution of thermostable kanamycin-resistance gene: a convenient selection marker for *Thermus thermophilus*. *J. Biochem. (Tokyo)* **126**, 951–956
21. Hashimoto, Y., Yano, T., Kuramitsu, S., and Kagamiyama, H. (2001) Disruption of *Thermus thermophilus* genes by homologous recombination using a thermostable kanamycin-resistant marker. *FEBS Lett.* **506**, 231–234
22. Yokoyama, S., Hirota, H., Kigawa, T., Yabuki, T., Shirouzu, M., Terada, T., Ito, Y., Matsuo, Y., Kuroda, Y., Nishimura, Y., Kyogoku, Y., Miki, K., Masui, R., and Kuramitsu, S. (2000) Structural genomics projects in Japan. *Nat. Struct. Biol.* **7**, 943–945
23. Yokoyama, S., Matsuo, Y., Hirota, H., Kigawa, T., Shirouzu, M., Kuroda, Y., Kurumizaka, H., Kawaguchi, S., Ito, Y., Shibata, T., Kainosho, M., Nishimura, Y., Inoue, Y., and Kuramitsu, S. (2000) Structural genomics projects in Japan. *Prog. Biophys. Mol. Biol.* **73**, 363–376
24. Dosanjh, M.K., Roy, R., Mitra, S., and Singer, B. (1994) 1,N6-ethenoadenine is preferred over 3-methyladenine as substrate by a cloned human N-methylpurine-DNA glycosylase (3-methyladenine-DNA glycosylase). *Biochemistry* **33**, 1624–1628
25. Newcombe, H.B. and Hawirko, R. (1949) Spontaneous mutation to streptomycin resistance and dependence in *Escherichia coli*. *J. Bacteriol.* **57**, 565–572
26. McCullough, A.K., Dodson, M.L., Scharer, O.D., and Lloyd, R.S. (1997) The role of base flipping in damage recognition and catalysis by T4 endonuclease V. *J. Biol. Chem.* **272**, 27210–27217
27. Roberts, A., Pelton, J.G., and Wemmer, D.E. (2006) Structural studies of MJ1529, an O^6-methylguanine-DNA methyltransferase. *Magn. Reson. Chem.* **44**, S71–S82
28. Takahashi, M., Sakumi, K., and Sekiguchi, M. (1990) Interaction of Ada protein with DNA examined by fluorescence anisotropy of the protein. *Biochemistry* **29**, 3431–3436
29. Chan, C.L., Wu, Z., Ciardelli, T., Eastman, A., and Bresnick, E. (1993) Kinetic and DNA-binding properties of recombinant human O^6-methylguanine-DNA methyltransferase. *Arch. Biochem. Biophys.* **300**, 193–200
30. Verdemato, P.E., Brannigan, J.A., Damblon, C., Zuccotto, F., Moody, P.C., and Lian, L.Y. (2000) DNA-binding mechanism of the *Escherichia coli* Ada O^6-alkylguanine-DNA alkyltransferase. *Nucleic Acids Res.* **28**, 3710–3718
31. Rasimas, J.J., Pegg, A.E., and Fried, M.G. (2003) DNA-binding mechanism of O^6-alkylguanine-DNA alkyltransferase. Effects of protein and DNA alkylation on complex stability. *J. Biol. Chem.* **278**, 7973–7980
32. Tamulaitis, G., Zaremba, M., Szczepanowski, R.H., Bochtler, M., and Siksnys, V. (2007) Nucleotide flipping by restriction enzymes analyzed by 2-aminopurine steady-state fluorescence. *Nucleic Acids Res.* **35**, 4792–4799
33. Samson, L., Thomale, J., and Rajewsky, M.F. (1988) Alternative pathways for the in vivo repair of O^6-alkylguanine and O^4-alkylthymine in *Escherichia coli*: the adaptive response and nucleotide excision repair. *EMBO J.* **7**, 2261–2267
34. Voigt, J.M., Van Houten, B., Sancar, A., and Topal, M.D. (1989) Repair of O^6-methylguanine by ABC excinuclease of *Escherichia coli* in vitro. *J. Biol. Chem.* **264**, 5172–5176
35. Edara, S., Kanugula, S., and Pegg, A.E. (1999) Expression of the inactive C145A mutant human O^6-alkylguanine-DNA alkyltransferase in *E.coli* increases cell killing and mutations by *N*-methyl-*N*′-nitro-*N*-nitrosoguanidine. *Carcinogenesis* **20**, 103–108
36. Selby, C.P. and Sancar, A. (1993) Molecular mechanism of transcription-repair coupling. *Science* **260**, 53–58
37. Selby, C.P., Witkin, E.M., and Sancar, A. (1991) *Escherichia coli mfd* mutant deficient in "mutation frequency decline" lacks strand-specific repair: in vitro complementation with purified coupling factor. *Proc. Natl Acad. Sci. USA* **88**, 11574–11578
38. Deaconescu, A.M., Chambers, A.L., Smith, A.J., Nickels, B.E., Hochschild, A., Savery, N.J., and Darst, S.A. (2005) Structural basis for bacterial transcription-coupled DNA repair. *Cell* **124**, 507–520
39. Ljungman, M. (2007) The transcription stress response. *Cell Cycle* **6**, 2252–2257
40. Viswanathan, A. and Doetsch, P.W. (1998) Effects of nonbulky DNA base damages on *Escherichia coli* RNA polymerase-mediated elongation and promoter clearance. *J. Biol. Chem.* **273**, 21276–21281